Sensors and Materials, Vol. 36, No. 9 (2024) 3779–3786
MYU Tokyo

S & M 3766

Sodium Aluminate Study in Response to Process Excursion

Wen-Cheng (Agingu) Shih*

Neogeneration Biotech Co., Ltd., 3F, No. 431, Dadun S. Rd., Nantun Dist., Taichung 408024, Taiwan

(Received April 12, 2024; accepted June 24, 2024)

Keywords: sodium aluminate, precipitation, sensor, phase diagram, titanium dioxide

The physical properties, the phase diagram for the Na_2O–Al_2O_3–H_2O system, and the crystal structure of sodium aluminate were studied. In laboratory-scale experimentally simulation tests, the undesired sodium aluminate solution precipitation served as a sensor for the excursion during the makeup process and/or in the storage state. For example, the feedstock for the subsequent hydrous alumina oxide deposition on pigmentary titanium oxide could be avoided and even restored. On the basis of the guide from the "modified" phase diagram, the abnormal composition of sodium aluminate was mapped and regressed to the baseline of Na_2O/Al_2O_3 with the mole ratio at 1.45, followed by the adjustment of water content through either water evaporation or water addition. The final required composition was recovered.

1. Introduction

Sodium aluminate has been the subject of intensive research using various physicochemical techniques over many decades owing to its commercial importance in the Bayer process for alumina manufacture,[1] TiO_2 processing,[2–4] and water treatment. Sodium aluminate belongs to the family of chemical compounds produced by the digestion of alumina trihydrate with caustic soda, with its chemical formula commonly written as $NaAlO_2$. However, its composition varies considerably, depending on the mole ratio (also called "caustic modulus" or "alpha") of Na_2O/Al_2O_3, where Na_2O is the synonym of NaOH. The chemical equation can be simply expressed as

$$Al_2O_3 \cdot 3H_2O + 2NaOH \rightarrow 2NaAlO_2 + 4H_2O.$$

The typical analytical results and properties of sodium aluminate are summarized in Table 1. The equilibrium diagram of the Na_2O–Al_2O_3–H_2O system[5] at 30 °C is shown in Fig. 1, demonstrating that the maximum solubility between two solid phases, namely, alumina trihydrate ($Al_2O_3{\cdot}3H_2O$) and sodium aluminate ($Na_2Al_2O_4{\cdot}2.5\ H_2O$), lies near 23% Al_2O_3 and 20% Na_2O. Qualitatively, a higher Na_2O concentration would favor the supersaturated solution, corresponding to $Na_2Al_2O_4{\cdot}2.5\ H_2O$, and a lower Na_2O concentration, i.e., a smaller amount of stabilized alkaline caustic, would result in the solution being saturated with respect to $Al_2O_3{\cdot}3H_2O$.

*Corresponding author: e-mail: agingu.shih@gmail.com
https://doi.org/10.18494/SAM5072

ISSN 0914-4935

Table 1
Typical analytical results and properties of sodium aluminate solution.

Color: Straw Colored to Light Amber Form: Liquid	
Na_2O/Al_2O_3 mole ratio	1.37
Specific gravity	1.51
wt% Al_2O_3	23.5
wt% Na_2O	19.6
Gram per liter (gpl) Al_2O_3	349.0
Gram per liter (gpl) Na_2O	296.0

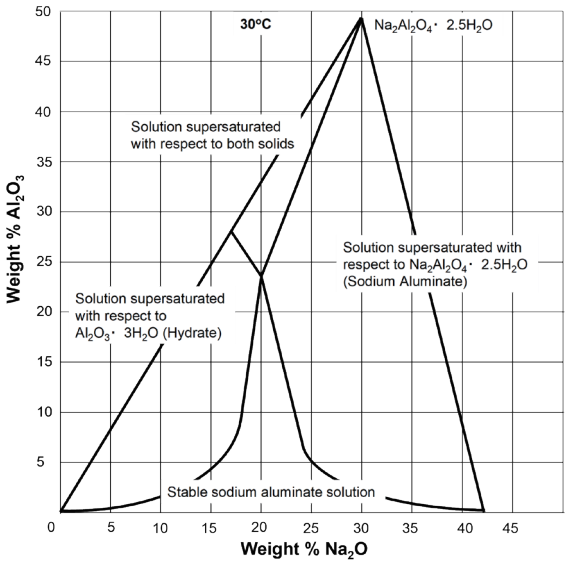

Fig. 1. Equilibrium diagram for Na_2O-Al_2O_3-H_2O system at 30 °C.

The structure of aluminate solutions has remained controversial since 1913. Thus, a large number of studies have been devoted to characterizing this alumina and hydroxide-ion-containing complex using many robust analytical techniques, including potentiometry, NMR, UV-visible spectroscopy, X-ray diffraction (XRD), and IR/Raman spectroscopy.[6–11] However, some structural discrepancies still remain owing to the lack of information from the individual techniques. The crystal structure of hydrated sodium aluminate was elucidated on the basis of the report by Kaduk and Pei[12] for $NaAlO_2 \cdot 5/4\ H_2O$. The basic unit is a single layer parallel to (001), composed of corner-sharing AlO_4 tetrahedra.

For example, the well-controlled sodium aluminate solution as the feedstock would ensure the appropriate hydrous alumina oxide surface coating for titanium dioxide processing in compliance with smooth manufacturing and consistent quality performance. Any deviation from the normal conditions from the feedstock would lead to undesirable consequences.

2. Data, Materials, and Methods

Laboratory work was conducted to determine the phase diagram for the Na_2O–Al_2O_3–H_2O system. Then, the precipitation area in the phase diagram was specifically defined by the thermodynamically observed sodium aluminate precipitation[13,14] after aging for different periods with mole ratios of 0.70, 0.91, 1.00, 1.30, 1.45 (baseline), 2.0, and 3.0, with varying wt% H_2O as shown in Table 2.

The well-defined phase diagram is shown in Fig. 2, where the gray area behaves similarly to a sensor for the undesired white precipitate in the sodium aluminate feedstock solution under abnormal excursion toward higher wt% H_2O, higher wt% Al_2O_3, and lower wt% Na_2O in comparison with the normal composition (red dot in Fig. 2). That is the area where the normal operation should avoid to ensure titanium oxide manufacturing and the resulting product with consistent quality in accordance with the required specifications.

Table 2
Different conditions for the Na_2O-Al_2O_3-H_2O system with and without the thermodynamically observed sodium aluminate precipitation.

Na_2O/Al_2O_3 (mole)	Sodium Aluminate (ml)	Added 45% NaOH (g)	Added Al_2O_3 (g)	Added H_2O (g)	Al_2O_3 (wt%)	Na_2O (wt%)	H_2O (wt%)	Precipitate
0.70	160	0	59.0	0	37.63	16.01	46.36	V[a]
0.70	160	0	59.0	40	33.23	14.14	52.63	V
0.70	160	0	59.0	80	29.76	12.66	57.58	V
0.91	160	0	33.0	0	31.76	17.52	50.72	V
1.00	160	0	25.0	−60	38.29	23.23	38.48	N/A[b]
1.00	160	0	25.0	−40	34.94	21.20	43.87	N/A
1.00	160	0	25.0	0	29.73	18.04	52.23	V
1.00	160	0	25.0	20	27.67	16.79	55.54	V
1.00	160	0	25.0	40	25.87	15.70	58.43	V
1.00	160	0	25.0	80	22.90	13.90	63.20	V
1.30	160	0	6.5	0	24.53	19.37	56.10	N/A
1.30	160	0	6.5	20	22.71	17.94	59.35	N/A
1.30	160	0	6.5	40	21.14	16.70	62.16	V
1.45	160	0	0	0	22.51	19.89	57.60	N/A
1.45	160	0	0	40	19.34	17.08	63.58	V
1.45	160	0	0	80	16.94	14.97	68.09	V
1.45	160	0	0	120	15.08	13.32	71.60	V
2.00	160	40.5	0	0	19.30	23.47	57.23	N/A
2.00	160	40.5	0	40	16.92	20.57	62.51	N/A
2.00	160	40.5	0	80	15.06	18.31	66.63	V
2.00	160	40.5	0	160	12.34	15.01	72.64	V
3.00	160	114.5	0	0	15.31	27.92	56.77	N/A
3.00	160	114.5	0	40	13.77	25.12	61.11	N/A
3.00	160	114.5	0	80	12.51	22.82	64.66	N/A
3.00	160	114.5	0	120	11.47	20.91	67.62	N/A
3.00	160	114.5	0	160	10.58	19.30	70.12	N/A
3.00	160	114.5	0	200	9.82	17.91	72.26	V

[a]V: with the thermodynamically observed sodium aluminate precipitation
[b]N/A: without the thermodynamically observed sodium aluminate precipitation

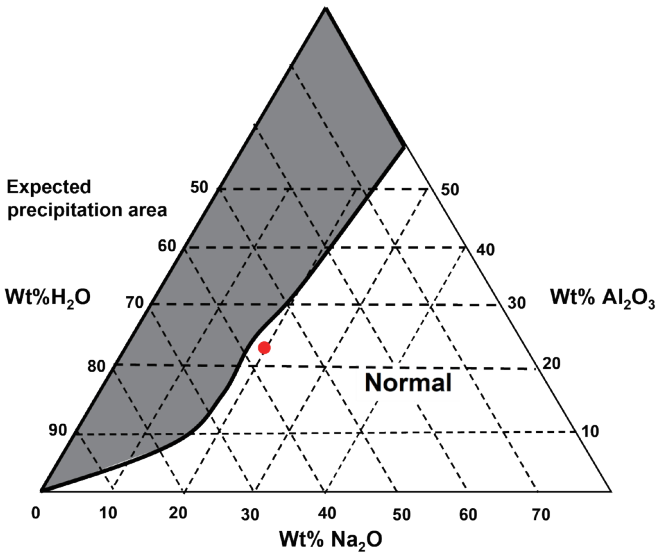

Fig. 2. (Color online) Well-defined Na_2O-Al_2O_3-H_2O phase diagram from the thermodynamically observed sodium aluminate precipitation.

Similarly to a sensor, the gray area was not physically activated directly. Instead, it triggered an alarm from the measurement data in terms of wt% Al_2O_3 and wt% Na_2O from the collected sodium aluminate solution. Any data that falls into the gray area of the phase diagram in Fig. 2 would trigger an alarm message to remind the operator to perform an immediate action that should be taken for recovery.

One of the alarm messages was activated during a sodium aluminate makeup process with the aim for gpl Na_2O at 300 (measured 165) and gpl Al_2O_3 at 335 (measured 244). Ultimately, this issue ended with the full recovery from an abnormal composition for sodium aluminate.

The sample with the major precipitated material from the sodium aluminate tank was subjected to composition measurement, suggesting that its composition is biased and misled by this data (point 0 in Fig. 3), owing to the composition analysis by acid-base titration for this sample with the major undissolved and precipitated Gibbsite $Al(OH)_3$. This analysis was only feasible for an aqueous solution sample. Then, the issued sample was poured into a 45% caustic solution to ensure the complete dissolution of the precipitate, providing the preliminary composition at point 1 in Fig. 3. While taking the deliberately added caustic solution into account, direct conversion to point 2 would indicate the original composition of this issued sample, demonstrating up to 58.78% Al_2O_3 with the major precipitation (aimed at 23.5%) and down to 9.08% Na_2O, with the Na_2O/Al_2O_3 mole ratio at 0.25 (aimed at 1.45). After appropriately mapping the abnormal composition, the first step was attempted to bring the issued sample back to the baseline from points 2 to 3. On the basis of the theoretical calculation from the phase diagram, it was suggested that a specific amount of the 45% caustic solution be poured into the tank first with the regression to point 3. Subsequently, a specific amount of water determined from the calculation was poured into the tank, moving downward from points 3 to 4 as shown in Fig. 3 with the full recovery.

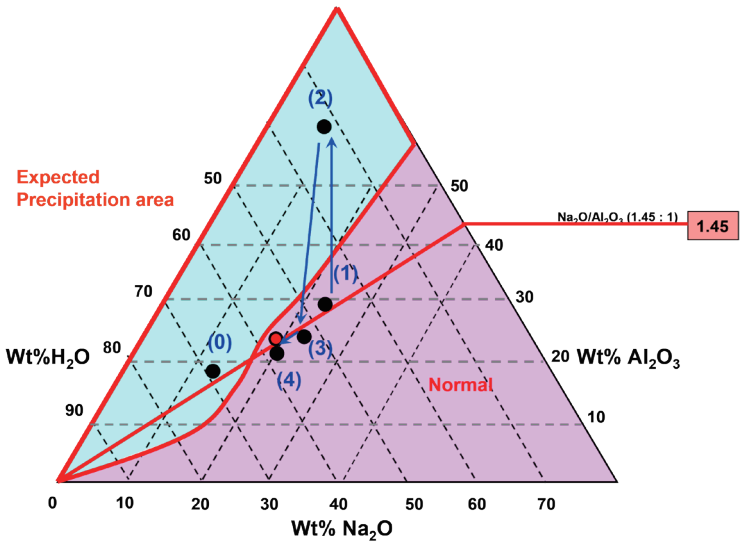

Fig. 3. (Color online) Composition in the phase diagram for the issued and normal sodium aluminate solution during the recovery course.

3. Results and Discussion

Five dried samples were subjected to structural characterization by XRD, as shown in Fig. 4, including the samples listed below,

(1) Aluminum trihydrate (gibbsite form), dry feedstock for sodium aluminate solution make-up
(2) Sodium aluminate: a solution aged at room temperature without a cap for a long period; a certain amount of water was vaporized with precipitate formation
(3) Sodium aluminate solution with the addition of 40% H_2O: 40% cold water was poured into a heated sodium aluminate solution and aged for a specified period (aluminum trihydrate, bayerite form) with the precipitate formation
(4) Sodium aluminate solution with the addition of acid: a sufficient amount of dilute HCl was added dropwise into the sodium aluminate solution (aluminum trihydrate, bayerite form) with the precipitate formation
(5) Sludge in the heel of the storage tank: sample from the suspended solid (a mixture of aged aluminum trihydrate, gibbsite form, and other exterior undefined species)

The sludge found in the heel of the storage tank was not freshly precipitated aluminum trihydrate. Instead, it was a mixture of aged aluminum trihydrate and other exterior undefined species, as corroborated by the XRD patterns shown in Fig. 4, where the major ingredient for the precipitate was in the gibbsite phase [Fig. 4(v)], instead of the bayerite phase, which can only be obtained by the addition of 40% water [Fig. 4(iii)] or enough acid [Fig. 4(iv)] to the normal sodium aluminate solution.

Following the Ostwald rule of the stage of alumina oxide formation, the less stable phase, namely, amorphous alumina, would be formed first, i.e., kinetically stable, followed by the phase transition to other stable phases with aging, i.e., thermodynamically stable. The phase can be seen in the following sequence:[13,14]

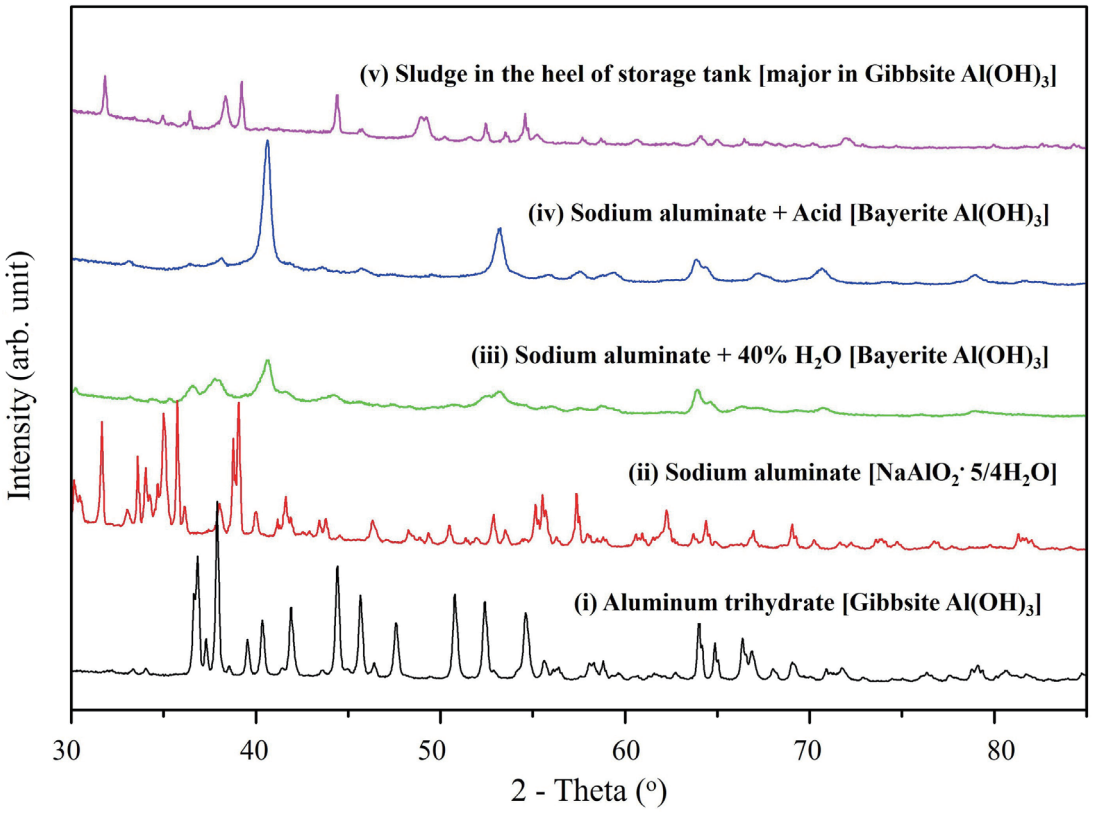

Fig. 4. (Color online) XRD patterns of all studied samples.

Amorphous ($Al_2O_3 \cdot nH_2O$) → Pseudo-boehmite [AlO(OH)] → Bayerite [$Al(OH_3)$] → Gibbsite [$Al(OH_3)$].

Noteworthy is that even normal sodium aluminate solution would precipitate slightly over time with primary heterogeneous nucleation on a foreign surface, such as the sides of the reaction tank or the blades of the agitator. Small scratches or pits on this surface can preferentially adsorb the precursor species, creating a high local concentration for nucleus formation, or air-exposed circulation from the pipeline back to the sodium aluminate storage tank, leading to a low local pH for a small amount of precipitate formed as seed.

Furthermore, the pH or concentration excursion of sodium aluminate solution, which would change the status of supersaturation, could lead to preformed hydrous alumina precipitation in the sodium aluminate storage tank.

An example has been made for pigmentary titanium dioxide processing with surface modification by hydrous metal oxide. For end-used product properties, the optical gloss is mostly the contribution from the required crystalline phase, whereas the durability performance is mostly achieved by the amorphous phase. The hydrous alumina oxide phase on the titanium oxide surface is strictly governed by the starting raw material, i.e., sodium aluminate solution, its concentration, the foreign ions present, the neutralization course/sequence, and temperature/

pH during the wet treatment manufacturing process, where the reaction between alkaline sodium aluminate and acidic HCl/H_2SO_4 would facilitate the precipitation of hydrous alumina oxide on titanium dioxide by bridging the surface hydroxyl group from the TiO_2 surface in the reaction tank. The crystalline phase can be precisely controlled by adjusting the reaction pH, temperature, and curing time at the wet treatment stage.

In general, the formation of metal oxide can proceed via the neutralization of specific metal salts in aqueous solution. Crystalline oxide would be developed via previously formed small charged molecules of water and metal ions, followed by direct growth and deposition on seed crystals after the neutralization, whereas amorphous oxide is formed from charged polymers, which are joined together with metal ions by oxide and hydroxide bridge bonding, followed by the precipitation of these charged polymers during neutralization. Experimentally, different types of hydrous alumina can be formed by different alumina precursors under certain pH and temperature conditions. When sodium aluminate in the form of monomeric species in solution is used as a precursor, crystalline boehmite (AlOOH) can be formed at 70 °C and pH 8.5, and crystalline gibbsite [alumina trihydrate: $Al(OH)_3$] can be formed at 70 °C and a slightly high pH of 10.5, whereas amorphous alumina can be obtained at 70 °C and both pHs 8.5 and 10.5 by another precursor of polymeric aluminum chloride hydroxide [$Al_2Cl(OH)_5$].

The gloss performance is improved using densely packed pigment particles through the presence of crystalline alumina oxide between TiO_2 pigments by reducing the van der Waals forces thereof in comparison with amorphous alumina oxide. In contrast, a complete and continuous surface coverage, e.g., amorphous alumina, would physically separate the paint binder and atmosphere oxygen/water from the TiO_2 pigment surface and impart the outperformed durability.

4. Conclusion

The defined phase diagram for the Na_2O–Al_2O_3–H_2O system can be used as not only the guide for abnormal process response/recovery, but as a sensor to prevent the formation of undesired precipitates from sodium aluminate solution. Any measured composition data of the prepared sodium aluminate solution that falls into the gray area of the phase diagram would trigger an alarm message to remind the operator to perform an immediate action that should be taken for recovery. Therefore, the excursion of abnormal composition of sodium aluminate can be recovered by mapping in the phase diagram and then the regression to the baseline of Na_2O/Al_2O_3 with the mole ratio at 1.45, followed by the adjustment of water content through either water evaporation or water addition.

Acknowledgments

I am deeply indebted to Dr. M. P. Diebold for his unremitting coaching and guidance regarding hydrous alumina chemistry. I also extend my special and heartfelt thanks to Agatha Lai and Kevin Huang for their excellent experimental work.

References

1 A. R. Hind, S. K. Bhargava, and S. C. Grocott: Colloids Surf. A **146** (1999) 359. https://doi.org/10.1016/S0927-7757(98)00798-5
2 N. Veronovski, M. Lešnik, and D. Verhovšek: J. Coat. Sci. Technol. **1** (2014) 51. http://dx.doi.org/10.6000/2369-3355.2014.01.01.6
3 N. Veronovski: J. Coat. Sci. Technol. **2** (2015) 6. https://doi.org/10.6000/2369-3355.2015.02.01.2
4 F. Ohashi: J. Coat. Technol. Res. **20** (2023) 1789. https://doi.org/10.1007/s11998-023-00794-3
5 A. S. Russell, J. D. Edwards, and C. S. Taylor: JOM **7** (1955) 1123. https://link.springer.com/article/10.1007/BF03377627
6 M. Weinberger, M. Schneider, W. H. Geßner, and D. Müller: ZAAC **621** (1995) 679.
7 G. Johansson: Acta Chem. Scand. **20** (1966) 505.
8 M. G. Barker, P. G. Gadd, and M. J. Begley: J. Chem. Soc., Chem. Commun. **8** (1981) 379. https://doi.org/10.1039/C39810000379
9 M. G. Barker, P. G. Gadd, and S. C. Wallwork: J. Chem. Soc., Chem. Commun. **9** (1982) 516. https://doi.org/10.1039/C39820000516
10 M. Weinberger, M. Schneider, V. Zabel, D. Müller, and W. Gessner: ZAAC **622** (1996) 1799.
11 G. Johansson, E. Dorm, M. Seleborg, K. Motzfeldt, O. Theander, and H. Flood: Acta Chem. Scand. **16** (1962) 403.
12 J. A. Kaduk and S. Pei: J. Solid State Chem. **115** (1995) 126. https://doi.org/10.1006/jssc.1995.1111
13 H. A. Van Straten, B. T. W. Holtkamp, and P. L. De Bruyn: J. Colloid Interface Sci. **98** (1984) 342.
14 H. A. Van Straten and P. L. De Bruyn: J. Colloid Interface Sci. **102** (1984) 260. https://doi.org/10.1016/0021-9797(84)90218-2

About the Authors

Wen-Cheng (Agingu) Shih received his Ph.D. degree from Taiwan University, Taiwan, in 2007. After that, he has played multiple roles in R&D, technical marketing, and operation in the titanium dioxide industry. His research interests are in heterogeneous catalysis and the surface modifications of inorganic oxide on pigments. (agingu.shih@gmail.com)